The role of terrestrial radiation in the generation of zonal and eddy available potential energy

By DONALD R. JOHNSON, *Department of Meteorology, University of Wisconsin*

(Manuscript received April 14, 1966)

ABSTRACT

Time averaged estimates of the generation of atmospheric zonal and eddy available potential energy by infrared radiation are obtained from 198 radiometersonde flights made at thirteen stations located in the eastern half of the United States and Caribbean Sea area. From the temperature and net radiation data the vertical profiles of temperature and atmospheric cooling are individually estimated by "least squares" approximating polynomials. A polynomial integration technique is developed to obtain the time averaged covariance of the cooling and temperature profiles for each of seven atmospheric layers. The time averaged estimates for each of the seven atmospheric layers are divided into transient, stationary eddy, and stationary zonal components. The results indicate that all are sinks of available potential energy with the estimates for the transient component being -0.13 watts/m^2, the stationary eddy being -0.08 watts/m^2, and the stationary zonal being -1.92 watts/m^2. An analysis of the daily values indicates that the transient generation varies considerably from day to day and at times attains large positive or negative values. The range of the transient generation estimates is slightly larger than the range of frictional dissipation estimates within the planetary boundary layer for light and moderate winds. There are pronounced vertical variations in the generation estimates with the extreme values, both positive and negative, occurring in the lower troposphere. This is undoubtedly the result of the varying distribution of cloudiness and water vapor. Because of the large daily variations as well as vertical variations, it appears that additional intensive studies of the generation for local disturbances should be undertaken. The implication of a positive infrared generation by the net heating component on a pressure surface is discussed.

1. Introduction

In 1955 Lorenz produced a mathematical model for the general circulation energetics by expanding Margules' (1903) concept of the separation of total potential energy into a portion not available for conversion into kinetic energy and a portion available for conversion. Lorenz (1955*a*) defines available potential energy as the difference between the total potential energy of an arbitrary atmosphere and that which would exist after adiabatic redistribution of the mass to a state of stable, horizontal density stratification. The available potential energy, which he partitions into zonal and eddy portions, is created by the differential heating or cooling of the atmosphere. From Lorenz's definition, the zonal portion is determined by the strength of the north-south thermal variance of the zonal mean temperature and is principally produced by the latitudinal covariance of zonal means of diabatic heating and temperature on a pressure surface. The eddy portion is a measure of the east-west thermal variance and is principally produced either indirectly by the action of the eddies on the zonal available potential energy or directly by the east-west covariance of diabatic heating and temperature on a pressure surface.

An implication of modern theory is that differential cooling may be equally as important as differential heating in the generation of available potential energy. Hence, the differential cooling of the atmosphere by long wave radiation, although always a sink of total potential energy, may be either a source or sink of available potential energy depending on the correlation between differential infrared cooling and the temperature field. Within the smaller scales of the secondary circulation the infrared cooling may generate eddy available potential energy.

For example, the warm cloudy regions of some cyclones lose less heat than cool clear regions of anticyclones, generating eddy available potential energy at this scale. Therefore, it seems important to consider the role that organized heating and temperature fields of the secondary circulation play in the generation of eddy available potential energy for the atmosphere's circulation.

In this paper the contribution of infrared cooling in the generation of zonal and eddy available potential energy is examined. Both the vertical and horizontal variations of cooling by infrared radiation are studied. Emphasis is placed on the role of the vertical variation of infrared cooling in the generation of eddy available potential energy and the design of a diagnostic model with sufficient resolution and reliability to estimate this quantity. Data from radiometersonde flights are used to obtain continuous profiles of temperature and net radiation. A polynomial technique is developed which permits the vertical integration of continuous profiles of infrared cooling and temperature. These integrals of the covariance of temperature and heating fields are used to estimate the height variation of the generation of eddy available potential energy within the atmosphere's secondary circulation.

Apart from scientific inquiry "to know," there is an economic justification for the determination of the contribution of infrared cooling in the generation of available potential energy. This need is primarily the result of recent scientific and engineering advances. One advance, the satellite, provides a means of determining the global coverage of heat sources and sinks within the atmosphere (Sabatini & Suomi, 1962; Smith, Horn & Johnson, 1966) while the other, the giant digital computer, provides the means of utilizing the satellite observations in expanded numerical weather prediction models which incorporate atmospheric heat sources and sinks. Thus, the immediate justification of this study is to determine if observations of infrared cooling are an item of information in an energetically consistent numerical model where the heat sources and sinks of potential energy balance the frictional dissipation of kinetic energy. From energy considerations it seems that infrared cooling information would be essential if the magnitude or the range of the generation of available potential energy is nearly equal to or greater than the magnitude or range of the frictional dissipation of kinetic energy.

2. Development and discussion of the physical model

The set of energy equations developed by Lorenz (1955a) for the exposition of the theory of available potential energy and the general circulation in pressure coordinates provides the framework upon which the physical model used in this study is based. To derive these equations from his expression for available potential energy in isentropic coordinates, Lorenz used two approximations—a binomial expansion and a horizontally fixed static stability. In another paper (1955b), he derives another set of equations for the time rate of change of available potential energy in isentropic coordinates including expressions for the generation and conversion without the introduction of these approximations. To my knowledge, estimates of the available potential energy in all diagnostic studies, including this paper, have been made using the approximate expressions in pressure coordinates with one exception (Dutton & Johnson, 1967). Subsequent to the completion of the research reported in this paper, Professor Dutton of Pennsylvania State University and the writer, using the generation expression in isentropic coordinates, determined a zonal generation estimate from heat budget data which, with respect to infrared processes, is noticeably different from the one presented in this paper. The divergence of the results is primarily due to a different scheme to determine by scales the importance of the processes of heat addition and is discussed in the results section. However, to reconcile the difference between the generation estimates in pressure and in isentropic coordinates, it is necessary and important to emphasize the relation between the two generation expressions that Lorenz presented. In this paper only the equations directly relating to the generation integral are presented and their physical significance discussed.

According to Lorenz (1955b), the generation of available potential energy, G_θ, for the mass of the atmosphere, M, is

$$G_\theta = \int_M [1 - (\tilde{p}/p)^{R/c_p}] Q \, dM \qquad (1)$$

where p is pressure, R is the specific gas constant for dry air, c_p is the specific heat at constant pressure, and Q is the rate of heat addition per unit mass. The θ subscript for G denotes Lorenz's generation integral determined from the use of isentropic coordinates while G without the subscript is the approximate expression in presure coordinates. The operator ($\sim$) represents an average over an isentropic surface with respect to its horizontal projection. In this expression, the generation is positive (negative) when the heat is added to an element of mass at a pressure greater (less) than the average pressure on the isentropic surface. It is also positive (negative) when the element of mass cools at a pressure less (greater) than its isentropic average pressure.

Using isobaric averages Lorenz represented (1) by

$$G_\theta = \int_M (\overline{\overline{N}}\,\overline{\overline{Q}} + \overline{N'' Q''})\, dM \tag{2}$$

where N is a weighting function of the integrand of (1) given by the square brackets. The operator ($\bar{\ }$) represents an average over a pressure surface taken with respect to its horizontal projection, while ($''$) represents a deviation from the average. Lorenz justified the approximation that

$$N'' = T''\Gamma_d(\Gamma_d - \overline{\overline{\Gamma}})\,\overline{\overline{T}} \tag{3}$$

where T is temperature, Γ_d is the dry adiabatic lapse rate and $\overline{\overline{\Gamma}}$ is the mean lapse rate of the horizontally averaged temperature field. He then stated that good estimates of the generation should be provided by the second term of the integrand of (2) which is approximately equal to the generation expression of his 1955a paper. However, he also noted that generation estimates from the approximate expression might suffer from the neglect of the first term of the integrand of (2) which represents a generation from net heating at high pressure and cooling at low pressure. In our study (Dutton & Johnson, 1967) the importance of this term is now apparent and its implication is discussed in the results section. In the intervening sections the emphasis is on (1) the role of infrared cooling in the generation of zonal and eddy available potential energy using Lorenz's approximate expression in pressure coordinates and (2) the development of numerical and statistical diagnostic techniques. The generation integral from the 1955a study must be regarded as that portion of the generation due to the covariance of temperature and heating on a pressure surface. The generation due to a net heating at high pressure and a net cooling at low pressure is not considered.

From Lorenz (1955a), the average generation of available potential energy per unit area of the earth's surface from the correlation of temperature and heating on a pressure surface is

$$G = \frac{1}{g}\int_0^{\overline{\overline{p}}_0} \frac{\Gamma_d}{(\Gamma_d - \overline{\overline{\Gamma}})\overline{\overline{T}}}\, \overline{\overline{T'' Q''}}\, dp \tag{4}$$

where g is the acceleration of gravity. Pressure is the independent variable serving as the vertical coordinate with boundary values $p = 0$ at the top of the atmosphere and $p = p_0$ at the earth's surface. In this representation the generation, G, of available potential energy is positive when, relative to horizontal averages on a pressure surface, the warmer air is heated and the colder air is cooled either increasing the horizontal variance of temperature and the store of available potential energy or immediately producing horizontal kinetic energy. The exact relationship of the generation of available potential energy and the average frictional dissipation, D, to the time rate of change of available potential energy, A, and the horizontal kinetic energy, K, is

$$\frac{\partial}{\partial t}(A + K) = G_\theta - D \tag{5}$$

The frictional dissipation integral, D, is regarded by Lorenz as the unique sink for kinetic energy; however, it is evident that the sum of the time rate of change of the available potential energy and kinetic energy is equal to the sources and sinks of both forms of energy. Thus in an open system differential heating may serve as a source or sink of horizontal kinetic energy, while the available potential energy for the atmosphere is a constant. Furthermore by disregarding friction, it is clear from equation (5) that positive (negative) generation causes an increase (decrease) in the sum of the two forms of energy.

Within the troposphere and lower stratosphere the generation of available potential energy can be attributed to five physical processes causing differential heating: 1) direct absorption by solar radiation, 2) emission of long wave radiation, 3) release of latent heat, 4) sensible heat transfer through the earth-atmosphere interface, and 5) frictional dissipation. Thus, the generation integral can be divided into five linear components corresponding to each physical process.

$$G = \sum_{i=1}^{5} G_i = \sum_{i=1}^{5} \frac{1}{g} \int_0^{\bar{p}_0} \frac{\Gamma_d}{(\Gamma_d - \bar{\bar{\Gamma}})\bar{\bar{T}}} \overline{\overline{T'' Q_i''}}\, dp \quad (6)$$

where the index, i, represents a physical process, and Q_i'' is the deviation of the rate of heat addition by the *i*th component from its horizontal mean, $\bar{Q}_i$. Furthermore, to separate the contribution of the systematic zonal heating field from the organized heating fields of other scales of atmospheric disturbances, following Lorenz the generation integral is divided into a zonal component and an eddy component. The zonal and eddy generation are further divided into a stationary and transient contribution by expressing the areal deviations as

$$T''_{(x,y,p,t)} = [\bar{T}]''_{(y,p)} + \bar{T}^*_{(x,y,p)} + (T')''_{(x,y,p,t)} \quad (7)$$

and

$$Q''_{(x,y,p,t)} = [\bar{Q}]''_{(y,p)} + \bar{Q}^*_{(x,y,p)} + (Q')''_{(x,y,p,t)} \quad (8)$$

where the brackets represent a zonal mean on a pressure surface and the asterisk a departure from a zonal mean. The operator ($^{-}$) represents a time average and a single prime (′) the deviation from a time average. The first and second terms on the right hand side of (7) and (8) are the time averaged stationary deviations while the third is the transient deviation. This partitioning is identical to that used by Murakami (1960) and discussed by Oort (1964). The substitution of equations (7) and (8) into (6) yields the following expression for the total time average generation

$$\bar{G} = \sum_{i=1}^{5} \bar{G}_i = \sum_{i=1}^{5} (G_{ZS_i} + G_{ES_i} + G_{T_i}) \quad (9)$$

where the order of integration for space and time are interchanged. Thus the time averaged generation, $\bar{G}$, is divided into three scales and five components of diabatic heating. The scales of atmospheric circulation are defined as follows:

$$G_{ZS} = \frac{1}{g} \int_0^{\bar{p}_0} \frac{\Gamma_d}{(\Gamma_d - \bar{\bar{\Gamma}})\bar{\bar{T}}} \overline{\overline{[\bar{T}]''[\bar{Q}]''}}\, dp \quad (10)$$

where G_{ZS} is the generation at the stationary zonal scale.

$$G_{ES} = \frac{1}{g} \int_0^{\bar{p}_0} \frac{\Gamma_d}{(\Gamma_d - \bar{\bar{\Gamma}})\bar{\bar{T}}} \overline{\overline{\bar{T}^* \bar{Q}^*}}\, dp \quad (11)$$

where G_{ES} is the generation at the stationary or standing eddy scale. It is associated with both the long planetary waves and continents or oceans, when the time interval of averaging is a few days. For longer time intervals, this term must be identified with stationary features due to the continents and oceans since even the long planetary waves are quasi-transient features of the atmospheric circulation.

$$G_T = \frac{1}{g} \int_0^{\bar{p}_0} \frac{\Gamma_d}{(\Gamma_d - \bar{\bar{\Gamma}})\bar{\bar{T}}} \overline{\overline{(T')''(Q')''}}\, dp \quad (12)$$

where G_T is the generation by the transient zonal scale associated with an expansion or contraction of the westerlies and the transient eddies primarily associated with surface cyclones, anti-cyclones or upper air traveling waves.

The total contributions to the generation by the five diabatic components at the various scales is still an unresolved problem. With regard to the overall generation at the eddy scale, Lorenz (1955*a*) states that "presumably it is negative, in view of the probable warming of cold air masses and cooling of warm air masses in middle latitudes, but the possible preference of warm longitudes for the release of latent heat may suppress this negative value". Although this postulate may be true, it is exceedingly difficult to verify or reject.

From diagnostics based on a quasi-geostrophic theory, Wiin-Nielsen & Brown (1962) estimated that the eddy generation by all physical processes is -3.5 watts/m² apparently confirming Lorenz's postulate.

Later Brown (1964), using the same model, obtained the following mean seasonal generation estimates; -2.4 watts/m² for January, -0.83 watts/m² for April, 1.25 watts/m² for July and -0.69 watts/m² for October. On the other hand, Clapp (1961) obtained an estimate of $+0.26$ watts/m² for the time averaged semipermanent circulation in winter.

In studies of the individual components, the positive generation by latent heat seems to have been well established by Palmén (1960), Clapp & Winninghoff (1963), and Murakami (1960).

Palmén estimated that an average of 53 watts/m^2 of kinetic energy was created for 1/35 of the polar cap north of latitude 30°N by the latent heat released in an intense extratropical cyclone (Hazel). From this estimate he stated that three extratropical disturbances of the same intensity as "Hazel" would suffice to produce the necessary kinetic energy to offset a frictional dissipation estimate of 5 watts/m^2 for the polar cap. Using data from one station (Washington, D.C.) Clapp (1963) estimated an eddy generation of 1.8 watts/m^2, the principal eddy generation component being the differential heating by the release of latent heat by thunderstorms. Since the summer thunderstorms at Washington, D.C. are usually identified with transient disturbances, Clapp's estimate does not contradict Murakami's (1960) estimate of 0.47 watts/m^2 for the eddy generation by the latent heat release in the stationary disturbances. One would expect transient disturbances to be more efficient than the stationary features in generating available potential energy, since the largest positive vertical velocities and greatest amounts of water vapor are found within the warm air of the transient scales. Thus, the large positive contribution due to the latent heat component provides support to Lorenz's qualifying statement that the release of latent heat might suppress the negative generation.

Another diabatic component that may generate a small amount of eddy available potential energy is the direct absorption of solar energy. Korb & Moller (1962) found that the direct solar absorption in warm, moist air may be twice as great as in clear, dry air. The presence of clouds in the warm, moist air increases the solar absorption. Since the greater heating occurs in the warm air, a positive generation results.

Merely from physical considerations, the component of differential heating by frictional dissipation can be dismissed as a negligible contribution. The total heating by frictional dissipation within the planetary boundary layer may reach several degrees per day; however, there does not appear to be any systematic effect leading to greater frictional heating in the warm air than in the cold air or vice versa.

Generation estimates of the remaining diabatic component, the cooling by infrared radiation have been established by the use of satellite measurements. Suomi & Shen (1963) obtained a mean generation of +0.583 watts/m^2 for 12 selected days of Explorer VII data. In a later analysis of 30 days of Explorer VII data, Shen's mean estimate (1963) was 0.260 watts/m^2. In a study of the generation associated with 500 mb waves using Tiros II data, Corcoran & Horn (1964) obtained a mean estimate of 0.055 watts/m^2. Although the latter two generation estimates are small, both studies indicated that at the smaller scale eddies the generation is approximately 0.2 watts/m^2, while the largest scales destroy available potential energy, approximately −0.1 watts/m^2. Thus, two tentative conclusions are: 1) cooling by radiation is not a large sink of eddy available potential energy and 2) generation of available potential energy by the infrared component is a function of scale size.

The positive generation within these smaller scale transient disturbances is undoubtedly the result of the distribution of clouds. Extensive cloudiness in the warm air, including the broad expanse of cirrus in the high troposphere ahead of the approaching wave, appreciably reduces the cooling by the infrared component. Within the cold, clear descending air of the disturbance the infrared radiation stream to space is a maximum. Thus, beneath the clouds, the warm air will cool less than will the cold air at corresponding heights. The result is an infrared contribution toward the positive generation of eddy available potential energy. Above the level of the clouds the horizontal differential heating fields are reversed (i.e., the warm air above the level of the clouds cools more than the cold air at equivalent heights). At these greater heights the eddy generation is then negative. Consequently, the vertical variation of the eddy generation of available potential energy by the infrared component may be an important element within a transient disturbance. In the next two sections, two polynomial techniques are developed and applied to radiometersonde data so that the vertical variation of the covariance of temperature and infrared cooling may be investigated and the generation by the infrared component estimated.

3. Procedures for estimating temperature and cooling profiles from radiometersonde data

As the result of instrumental developments during the last decade, measurements of the

Table 1. *Radiometersonde stations*

Index No.	Station	Location
Zone I (38.5°–51.5° N)		
72405	Washington, D.C.	38°–51″ N—77°–02″ W
72532	Peoria, Illinois	40°–40″ N—89°–41″ W
72641	Madison, Wisconsin	43°–08″ N—89°–24″ W
72645	Green Bay, Wisconsin	44°–29″ N—88°–08″ W
72747	International Falls, Minnesota	48°–34″ N—93°–26″ W
Zone II (25.5°–38.5° N)		
72202	Miami, Florida	25°–49″ N—80°–17″ W
72226	Montgomery, Alabama	32°–18″ N—86°–24″ W
72363	Amarillo, Texas	35°–14″ N—101°–42″ W
Zone III (12.5°–25.5° N)		
78383	Grand Cayman, Cayman Islands	19°–15″ N—85°–25″ W
78525	San Juan, Puerto Rico	18°–28″ N—66°–07″ W
78866	Phillipsburg, St. Martin	18°–02″ N—63°–06″ W
78967	Chagmaramus Bay, Trinidad	10°–11″ N—61°–37″ W
78988	Willemstad, Curacao	12°–11″ N—68°–59″ W

vertical distribution of the flux of infrared radiation have become feasible. Concurrently with the radiation measurements by Brewer & Houghton (1956) and Gergen (1956), the Suomi-Kuhn (1958) balloon-borne net radiometersonde was developed at the University of Wisconsin to provide measurements of the upward, downward, and net flux of infrared radiation. Radiometersonde flights conducted during the last nine years have provided data for research into the nature of the infrared cooling of the atmosphere.

From this nine year period, the only data sample providing adequate coverage to study the generation of available potential energy consists of the 198 individual night time flights made during December, 1960 and January, 1961. These flights were conducted by thirteen radiometersonde stations over the eastern half of the United States and the Caribbean. The radiometersonde flights provided discrete observations of temperature, net radiation, and pressure at approximately 600–800 foot intervals of height. Only nocturnal flights were made in order to avoid direct solar heating of the radiometersonde's infrared sensors. In Table 1, the stations, their locations and an identifying zonal ring are given, while Table 2 presents the date of each flight. Although there are missing observations in the time series for each station, this is not a serious defect since only time averaged estimates will be considered in this study.

To apply the radiometersonde data to the problem at hand, several statistical techniques were developed. Because some of the techniques require lengthy proofs, they were developed as five separate appendices in the original thesis (Johnson, 1965). The first was to obtain accurate profiles of temperature and cooling. The second was to develop a method of integration using a polynomial description for the temperature and cooling profiles. Previous generation studies employed satellite infrared radiation measurements. As a result, the generation integral was evaluated by assuming that a vertical mean value for the temperature and the cooling profiles was representative of their vertical distribution within an entire atmospheric unit column, thus ignoring the height dependency of both variables. Since a systematic height dependency exists for both the temperature and the heating fields, it is quite probable that the correlation between temperature and atmospheric cooling is not a constant in the vertical but will also vary as a function of height (Clapp & Winninghoff, 1963). To avoid the use of mean values, a diagnostic model was designed in which the generation of available potential energy is evaluated by dividing the atmosphere into seven levels. Within these

Table 2. *Observational dates of radiometersonde flights (0000Z)*

	December 1960									January 1961															
Station	20	21	22	23	24	25	26	27	28	7	8	9	10	11	12	13	14	15	16	17	18	19	20	21	Total
Zone I																									
405	×	×	×	×	×		×	×	×	×	×	×	×	×	×	×	×	×		×	×				19
532	×		×	×	×	×				×	×	×	×	×	×	×	×	×		×	×				16
641				×					×			×		×	×										6
645																×	×	×	×	×	×	×	×	×	9
747	×	×	×	×	×	×			×	×	×	×	×	×	×	×	×	×	×	×	×				19
Zone II																									
202									×	×	×	×		×	×	×	×		×						9
226		×	×	×			×		×	×	×	×	×	×	×		×	×	×	×	×	×			17
363			×	×	×	×	×			×	×	×	×	×			×	×	×	×	×	×			16
Zone III																									
383	×	×	×	×	×	×	×	×	×	×	×	×	×	×	×	×	×	×	×	×					20
525		×	×	×	×	×	×	×		×	×	×	×	×			×	×	×	×	×	×	×		19
866	×	×		×	×	×	×	×	×		×	×	×	×	×	×	×	×	×						17
967			×	×	×		×	×	×					×	×			×	×	×					11
988	×	×	×	×	×	×	×	×	×		×	×	×	×	×	×	×	×	×	×	×				20

seven levels, the temperature and infrared cooling profiles are described by approximating polynomials and the correlation between the two fields is then integrated.

As previously noted, the data used are air temperature and net radiation observations, which are the dependent variables, and the pressure observation, which is the independent variable. Since these measurements involve several sources of error, one must regard each observation as being composed of a true function on which is superimposed an instrumental error component. Thus let

$$y_i = \eta_i + \varepsilon_i \tag{13}$$

where y_i is the ith observation of the true function, η_i, and ε_i is the instrumental error component. If the observations are biased, then the expected value of the instrumental error is

$$E(\varepsilon_i) = \lambda_i \tag{14}$$

and

$$y_i = \eta_i + \lambda_i + \varepsilon_{Ri} \tag{15}$$

where λ_i is the bias component and ε_{Ri} is the random error component with expectation zero. It is the random error component of the observations of net radiation which causes the computational problem, since the estimation of atmospheric cooling from the observation of net radiation is obtained from second differences. The air temperature and pressure observations are used directly and do not present any computational difficulties. Since pressure is used as an independent variable, it is regarded as an exact measurement, allowing cooling rates to be efficiently estimated. The effect of this assumption is discussed at the end of this chapter. Because the estimation of temperature profiles follows directly from the techniques and criteria developed in solving the infrared cooling problem, the method of estimating temperature profiles is discussed after the procedure for estimating vertical profiles of cooling is developed.

The observations of net radiation are a combination of two temperature measurements by a top and a bottom sensor of the radiometer (Suomi, Staley, and Kuhn, 1958). In a study of the effects of temperature errors on radiation estimates (Johnson, 1966), the validity of regarding the net radiation observation as being a measurement of a smooth true function with a superimposed random error component is established. Thus the net radiative flux is

$$R_n = \gamma_n + \lambda_n + \varepsilon_{nR} \tag{16}$$

where γ_n is a linear combination of the two true temperature functions, λ_n is a linear combination of all bias error terms, ε_{n_R} is a linear combination of the random error components and the subscript n denotes net radiation variables.

The local cooling or warming of an atmospheric layer due to the divergence of infrared radiation is given by

$$Q = g\frac{\partial R_n}{\partial p} \quad (17)$$

where Q is the rate of addition of heat per unit mass. Substitution of (16) into (17) yields

$$Q = g\frac{\partial}{\partial p}(\gamma_n + \lambda_n + \varepsilon_{n_R}) \quad (18)$$

While one wishes to estimate the vertical derivative, $\partial\gamma_n/\partial p$, but is possibly forced to estimate $\partial/\partial p(\gamma_n + \lambda_n)$, a biased estimate, the optimum estimates of either derivative will be provided by filtering the random component before any form of differentiation is attempted (Hildebrand, 1956).

Since the data contain a random error component, "least squares" approximating polynomials rather than an exact polynomial description were selected for the filtering. With an approximating polynomial the estimating function is free to determine a new point at each level of the independent variable, thus avoiding consequences of an exact polynomial fit (i.e., the determination of an estimating function which passes through each observation but oscillates about the true function). Furthermore, any attempt to differentiate an exact polynomial description of net radiation to determine cooling by equation (18) would only amplify the oscillations due to the random error component and would prevent any form of convergence to the true profile $\partial\gamma_n/\partial p$.

The approximating polynomial estimate for the ith observation of net radiation is

$$\hat{R}_{n_i} = B_0 + B_1 x_i + \cdots B_k x_i^k. \quad (19)$$

The scaled independent variable of pressure, x_i, within each atmospheric layer is

$$\left.\begin{aligned} x_i &= \frac{p_i - \frac{1}{2}(p_{s+1} + p_s)}{\frac{1}{2}(p_{s+1} - p_s)} & p_s \geqslant p \geqslant p_{s+1} \\ x_i &= \frac{p_i - c_{1s}}{c_{2s}} & -1 \leqslant x \leqslant +1 \end{aligned}\right\} \quad (20)$$

where c_{1s} is the mean value and c_{2s} is one-half the range of the pressure interval, p_s to p_{s+1}. The independent variable was scaled to range between -1 and $+1$ for the atmospheric layer (Plackett, 1960). In matrix notation

$$\hat{\mathbf{R}}_n = \mathbf{X}\,\mathbf{B} \quad (21)$$

where $\hat{\mathbf{R}}_n$ is the $n \times 1$ vector of predicted values of net radiation for the n observations of net radiation within each atmospheric layer, $\mathbf{X}$ is the $n \times (k+1)$ design matrix of the independent variable, and $\mathbf{B}$ is the $(k+1) \times 1$ vector of polynomial coefficients. The solution to the polynomial coefficients is

$$\mathbf{B} = [\mathbf{X}^T\mathbf{X}]^{-1}\mathbf{X}^T\mathbf{R}_n \quad (22)$$

where $\mathbf{R}_n$ is the $n \times 1$ vector of observations for each atmospheric layer. The relation of the predicted values to the observed values is given by substituting equation (22) into (21) yielding

$$\hat{\mathbf{R}}_n = \mathbf{X}[\mathbf{X}^T\mathbf{X}]^{-1}\mathbf{X}^T\mathbf{R}_n \quad (23)$$

Thus, the predicted values for the net radiation are a linear transformation of the observations.

If the approximating polynomial is unbiased, the relation between the true function $(\gamma_n + \lambda_n)$ and the expected value of the polynomial coefficient is

$$(\boldsymbol{\gamma}_n + \boldsymbol{\lambda}_n) = \mathbf{X}E(\mathbf{B}) \quad (24)$$

From equations (21), (22) and (24), the expected value of R_n is

$$E(\hat{\mathbf{R}}_n) = (\boldsymbol{\gamma}_n + \boldsymbol{\lambda}_n) \quad (25)$$

From this equation it is evident that even though the approximating polynomial is an unbiased estimate of the ith observation, R_{n_i}, the predicted values, $\hat{R}_{n_i}$, are really estimating the function $(\gamma_{n_i} + \lambda_{n_i})$. Thus, if the approximating polynomial is unbiased, and since it is a linear transformation of the observations, one may use Gauss' Theorem (Kendall & Stuart, 1961) to state "of all the possible linear transformations, the estimates of R_n are minimum variance estimates for net radiative flux $(\gamma_{n_i} + \lambda_{n_i})$." (Johnson, 1965). It is logical to extend the argument, primarily because of this theorem, and state that a net radiative flux estimate by an unbiased approximating polynomial is the best linear estimate of the true continuous function $(\gamma_n + \lambda_n)$.

Before proceeding further, let us distinguish between the two bias errors in order to establish their effect on the estimation of the cooling profiles. The first, the bias error of measurement λ_n of equation (16) is a combination of the bias errors in the temperature measurements and the neglect of high order terms in defining a set of equations for the radiometersonde (Suomi, Staley and Kuhn, 1958). The second, the bias error due to "lack of fit" of the approximating polynomials to the observations within the atmospheric layer, is from either the improper selection of an rth degree polynomial for the unbiased kth degree polynomial, or from the choice of an atmospheric layer so large that the functional form of R_n cannot be adequately represented by an approximating polynomial. Since the approximating polynomial attempts to fit $(\gamma_n + \lambda_n)$, the expected value of R_n with a bias term due to lack of fit is

$$E(\hat{R}_n) = (\gamma_n + \lambda_n) + \lambda_B \tag{26}$$

where λ_B is the systematic bias error from the lack of fit. Defining the relation between the true function of cooling, χ, and the vertical distribution of the true net radiative flux to be

$$\chi = g\frac{\partial \gamma_n}{\partial p} \tag{27}$$

the substitution of the expected values of $\hat{R}_n$ from (26) for R_n of (17) in the equation for cooling yields

$$E(Q) = \chi + g\left(\frac{\partial \gamma_n}{\partial p} + \frac{\partial \lambda_B}{\partial p}\right) \tag{28}$$

Thus, it is clear that both bias errors will cause errors in the estimation of cooling rates. In considering the effect of the first bias error, the experimental work of Bushnell (1962) indicates that instrumental bias errors are negligible at pressures greater than 30 mb. It is important to note that any bias error in the telemetry system of the radiometersonde will have a negligible influence on estimates of net radiation since the bias errors in the top and bottom temperature measurements cancel each other (Johnson, 1966). For a constant bias error of either sensor, cooling estimates are unbiased since the derivative, $\partial\lambda_n/\partial p$, is zero. Furthermore, if a systematic bias error exists which is a function of pressure only, the generation estimates will not be influenced, for when subtracting to determine the field of heating deviations the bias errors of both the mean profile and arbitrary profiles cancel each other. Therefore, the possibility of any bias error in the measurements affecting the estimates of the generation of the available potential energy is dismissed.

The possibility of the second bias error, the lack of fit, is minimized by satisfying several criteria (Johnson, 1965). Briefly, these criteria are: 1) the selection of a "region of immediate interest" from the entire function, γ_n, so that within this region R_n may be described by a low order unbiased kth degree polynomial, 2) the RMS error estimate from the residual sums of squares of the unbiased kth degree polynomial is nearly equal to the RMS error estimate determined from a laboratory or a replicated experiment, and 3) the number of observations within the "region of immediate interest" is large compared to the degree, k.

The first criterion is partially satisfied by dividing the atmosphere into seven layers. This division is both meteorologically and statistically sound since the generation may be studied as a function of height and the entire span of pressure is reduced to several "regions of immediate interest". Within each "region of immediate interest" the appropriate unbiased kth order polynomial is selected by comparing the estimates of error variance, $\hat{\sigma}_R^2$, of the 0th through the 4th degree polynomials.

$$\hat{\sigma}_R^2 = \frac{(\mathbf{R}_n - \hat{\mathbf{R}}_n)^T (\mathbf{R}_n - \hat{\mathbf{R}}_n)}{n - (r+1)} \tag{29}$$

Here, n in the denominator is the number of observations and r the appropriate degree. In the first test, each estimate of the error variance by the rth degree polynomial was compared with the $(r+1)$th degree for polynomial orders zero through four. If the estimate r was less than the estimate $(r+1)$, the rth degree was selected as the optimum kth degree, provided it satisfied appropriate tests for criteria two and three. The specific criteria chosen were that the estimate of the error variance for the kth degree polynomial would not exceed 4.00×10^{-4} ly²/min² ($\hat{\sigma}_R = 0.020$ ly/min) and that the number of observations within the layer would exceed $4(r+1)$. The upper limit of $\hat{\sigma}_R^2$, allowing for sampling variations, is based on Bushnell's estimate (1962) of 0.36×10^{-4} ly^2/min^2 ($\hat{\sigma}_R = 0.006$) for the random error variance. In these results the lowest order rth degree polynomial satisfying these tests is selected as the optimum kth degree polynomial. If no local minimum for $\hat{\sigma}_R^2$ occurs, the 4th degree is selected provided criteria two and three are satisfied; otherwise, the layer is rejected. However, in 86 per cent of the layers, an optimum degree was selected by the test for a local minimum. The local minimum for $\hat{\sigma}_R^2$ as a function of r in (29) occurs when the rate of the monotonically decreasing numerator is insufficient to offset the influence of the denominator for each higher $(r+1)$th degree. In this study the unbiased estimate of the error variance, $\hat{\sigma}_R^2$, served as an excellent discriminator for the selection of the appropriate kth degree unbiased approximating polynomial. It should also be noted that all layers contained more than ten points since the three observations outside of the layer but adjacent to the upper and lower boundaries were included. This was necessary to achieve continuity for the estimate of cooling across the boundaries. Furthermore, the highest layer used in each flight was required to have at least three observations above its boundary.

After the selection of the kth degree polynomial as the best estimate of R_n over the "region of immediate interest," the polynomial is differentiated.

$$\frac{\partial \hat{R}_n}{\partial p} = \frac{\partial x}{\partial p}(B_1 + 2B_2 x + \cdots kB_k x^{k-1}) \tag{30}$$

In matrix notation the $n \times 1$ vector of derivatives of the net radiative flux is

$$\frac{\partial \hat{\mathbf{R}}_n}{\partial p} = c_{2s}^{-1}\,\mathbf{XCB} \tag{31}$$

where $\mathbf{C}$ is a $(k+1)$ diagonal matrix with diagonal elements, ii, given by $(i-l)/x$ for $i = 1, \dots, (k+1)$. The $n \times 1$ vector of cooling estimates from equation (17) is

$$\mathbf{Q} = g\frac{\partial \hat{\mathbf{R}}_n}{\partial p} \tag{32}$$

where $\mathbf{Q}$ is a $n \times 1$ vector of the estimate of infrared cooling (i.e., rate of addition of heat per unit mass). Substitution of equation (22), and (31) into (34) yields

$$\mathbf{Q} = gc_{2s}^{-1}\,\mathbf{XC}[\mathbf{X}^T\mathbf{X}]^{-1}\,\mathbf{X}^T\mathbf{R}_n \tag{33}$$

Since the infrared cooling estimates are linearly related to the observations of net radiation, one may again use Gauss' Theorem to state, "of all the possible linear transformations for the 'immediate region of interest,' the estimates of Q by the unbiased kth degree polynomial are minimum variance estimates for infrared cooling." (Johnson, 1965). From Johnson (1965), an important property of derivative estimates by a differentiated unbiased approximating polynomial is that the derivative estimates are also unbiased. Thus the expected value of equation (31) for an unbiased approximating polynomial is

$$E\left(\frac{\partial \hat{\mathbf{R}}_n}{\partial p}\right) = \frac{\partial \Upsilon_n}{\partial p} \tag{34}$$

and the expected value of the infrared cooling estimates by equations (32) and (33) is

$$E(\mathbf{Q}) = \chi \tag{35}$$

Thus, the infrared cooling estimates from unbiased approximating polynomials and unbiased observations are also unbiased.

The criteria for the estimation of infrared cooling were developed by analyzing atmospheric cross-sections from International Falls to Curacao, Venezuela, for January 7 and 9, 1961. In the analysis, using estimates by this method, the tests leading to the three criteria provided consistent profiles of atmospheric cooling. The critical factors necessary to provide consistent estimates were: 1) an estimate of error variance nearly equal to the estimate by Bushnell (1962), and 2) a greater number of observations within each atmospheric layer as the order, k, of the unbiased approximating polynomial increased.

Estimates of the random error variance of atmospheric cooling estimates were determined by comparing individual estimates from the net radiation observations from a "doubleheader" radiometersonde flight conducted on 1 February 1962 at Madison, Wisconsin in which the telemetry system alternately transmitted observations from the two radiometers mounted on the same radiosonde. From this method one can determine not only an estimate for the variance but more important, whether the technique developed in this chapter and applied separately to data from each radiometer provides consistent estimates for the true profiles of atmospheric cooling.

The kth degree polynomial for each layer was determined from the data for each radiometer and was used to individually estimate the true continuous cooling profiles. In Figure 1, an example of the technique for estimating the approximating polynomial profiles of net radiation for the 100–50 mb layer of the doubleheader flight is presented. The left-hand ordinate is the scaled variable of pressure. The curves are different kth degree polynomial representations of the two series of discrete observational estimates from each radiometer and are determined independently. This layer was selected for the example to show the consistency of the net radiation estimates between radiometer I and radiometer II even though the technique of determining the appropriate kth degree for each observational series selected two different degrees. Identical degrees were selected for four of seven layers of the doubleheader flight.

In Figure 2, the cooling estimates by the differentiated polynomials are presented. After differentiation of the net radiation polynomials, the estimates of infrared cooling are given by a third degree polynomial from radiometer I and by a first degree polynomial from radiometer II. Note the close agreement of the profiles when one considers that the infrared cooling estimates range from $-10°C/day$ to $+5°C/day$. The discrete values of infrared cooling estimated from adjacent values of net radiation by a finite approximation are presented to demonstrate the dominating effects of observational noise. Realistic profiles can only be obtained by computing average values of cooling for larger pressure intervals or by the differentiated polynomial technique. A description of the polynomial filtering technique presently used for the routine data processing of radiometersonde flights and developed from these results is described by Kuhn and Johnson (1966).

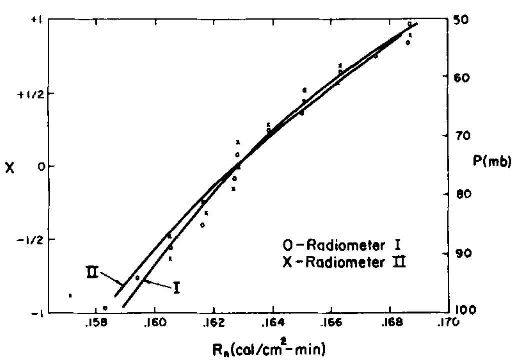

Fig. 1. Net radiative flux polynomial and finite estimates from the doubleheader radiometer flight.

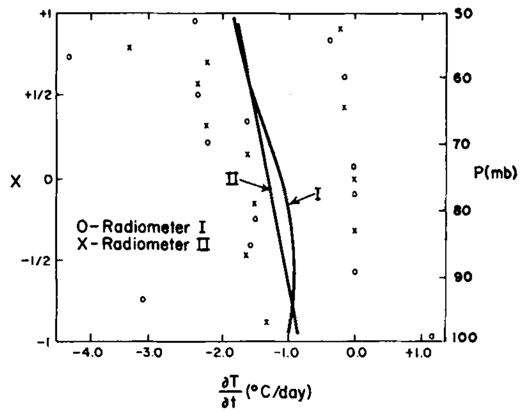

Fig. 2. Differentiated polynomial and finite derivative estimates of atmospheric cooling from the doubleheader radiometer flight.

In the doubleheader radiometer flight, the maximum estimate of cooling was $-3.2°C/day$ at 310 mb and the minimum estimate $+0.6°C/day$ at 470 mb. The averaged RMS estimate of the error obtained by the differences between the two cooling curves at 25 mb intervals at pressures greater than 100 mb and at 10 mb intervals at pressures less than 100 mb is $\pm 0.22°C/day$. This RMS estimate by this method can be compared with Kuhn's RMS estimate (1961) of 0.34°C/day for the mean cooling of a 100 mb layer. Thus, the polynomial technique provides continuous estimates of the vertical profile of atmospheric cooling with greater reliability and avoids the overly smooth mean estimates by 100 mb finite differences. This improvement in estimation of atmospheric cooling rates is due to the utilization of all the information from the observations within the "region of immediate interest" and the ability of the "least squares" method to redistribute the random error component of each observation over a predicted function in a manner similar to its superposition on the measurements of the true function.

The estimates of the temperature profiles were also determined by approximating polynomials; however, the criteria determining the kth degree unbiased polynomials were not as

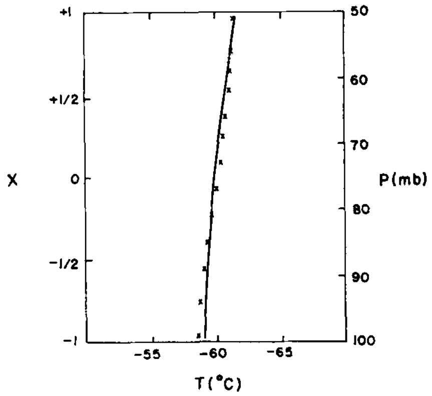

Fig. 3. Polynomial estimate and observed values of the free air temperature from the doubleheader radiometer flight.

stringent. Only polynomial orders through the second degree were compared to determine if a local minimum for the estimate of the random error variance occurred before the second degree, since the description by a second order polynomial was sufficient to describe the vertical variation of temperature within each atmospheric layer. If a local minimum occurred, the 0th or 1st degree became the kth degree polynomial, however, if not, the second degree was used as the kth order unbiased estimate provided that the RMS error estimate was less than 4°C. The latter test was necessary to determine errors resulting from faulty data processing. The nearly perfect description of the temperature profile is indicated by the value of the RMS error estimate from the residual sums of squares. This estimate was usually between ± 0.3 to ± 0.4°C, a value close to the random instrumental error component of air temperature (AWS TR-105-133, 1955). The polynomial profile and the discrete observations of temperature for the same 100–50 mb layer of the doubleheader in radiometersonde flight are presented in Figure 3 to illustrate a representative result. Although in this study pressure is regarded as an exact measurement, in reality there exists a small error component in the observation. Consequently, this effect reduces the magnitude of the regression coefficients (Kendall & Stuart, 1961) of both the approximating polynomials for net radiation and temperature, causing the variation in the profiles to be slightly underestimated. However, since the RMS error is approximately ± 0.3 mb while the range of atmospheric pressure for each layer is at least 25 mb, this effect can be disregarded as negligible.

4. Generation estimates by approximating polynomial integrals

In the previous section it was shown that approximating polynomials can be used to provide consistent estimates of temperature and cooling profiles. Since the polynomial coefficients may be averaged to provide the space and time means from which the deviations of temperature and infrared cooling are determined, estimates of Lorenz's generation integral as a function of height can be obtained for the generation at the various scales of atmospheric circulation. To realize this advantage, a diagnostic model is designed which incorporates the polynomial coefficients into a method of integration. Integration over each of the seven layers describes the vertical distribution of the generation of available potential energy. The diagnostic model is based on the technique of integrating two polynomial functions. General development of this technique is presented in Appendix V of the original thesis (Johnson 1965).

The predicted polynomial functions for temperature (T) and the rate of heat addition (Q) for an arbitrary atmospheric layer may be expressed as

$$\hat{T} = \mathbf{x}_1 \mathbf{A} \tag{36}$$

$$\hat{Q} = g \frac{\partial x}{\partial p} \mathbf{x}_2 \mathbf{C} \mathbf{B} \tag{37}$$

where $\mathbf{A}$ and $\mathbf{B}$ are $(k+1) \times 1$ and $(q+1) \times 1$ vectors of unbiased polynomial coefficients, $\mathbf{x}_1$ and $\mathbf{x}_2$ are the corresponding $1 \times (k+1)$ and $1 \times (q+1)$ vectors of the powers of the independent variables $[1, x, x^2, \ldots, x^k]$. The space averaged profiles of (36) and (37) are

$$\bar{\hat{T}} = \mathbf{x}_1 \bar{\mathbf{A}} \tag{38}$$

$$\bar{\hat{Q}} = \mathbf{x}_3 \bar{\mathbf{B}} \tag{39}$$

where the vector $\mathbf{x}_3$ is equal to the vector $[g(\partial x/\partial p)\mathbf{x}_2 \mathbf{C}]$ of equation (37), and the space deviations are

$$\hat{T}'' = \mathbf{x}_1(\mathbf{A} - \bar{\mathbf{A}}) = \mathbf{x}_1 \mathbf{A}'' \tag{40}$$

$$\hat{Q}'' = \mathbf{x}_3(\mathbf{B} - \bar{\mathbf{B}}) = \mathbf{x}_3 \mathbf{B}'' \tag{41}$$

Substitution of (40) and (41) into the generation integral (4) yields

$$G = \frac{1}{g}\sum_{s=1}^{7}\int_{p_{s+1}}^{p_s}\frac{\Gamma_d}{(\Gamma_d-\overline{\Gamma}_s)\overline{T}_s}\overline{\overline{A_s''^T \mathbf{x}_1^T \mathbf{x}_s B_s''}}\,dp \quad (42)$$

where the atmosphere is divided into seven layers ($s = 1, \ldots, 7$). For an atmosphere in local hydrostatic equilibrium and possessing a linear lapse rate, the horizontally averaged temperature profile within an arbitrary layer, s, is

$$\overline{T}_s = \overline{T}_{0s}\left(\frac{p}{p_{0s}}\right)^{R\overline{\overline{\Gamma}}_s/g} \quad (43)$$

where T_{0s} and p_{0s} are the lower boundary values of temperatures and pressures and $\overline{\overline{\Gamma}}_s$ is the lapse rate. Substituting (43) into (42) gives

$$G = \frac{1}{g}\sum_{s=1}^{7}\frac{(p_{0s})^{R\overline{\overline{\Gamma}}_s/g}}{(1-\overline{\overline{\Gamma}}_s/\Gamma_d)\overline{T}_{0s}}$$

$$\times\ \overline{\overline{\mathbf{A}_s''^T\left\{\int_{p_{s+1}}^{p_s} p^{-R\overline{\overline{\Gamma}}_s/g}\mathbf{x}_1^T\mathbf{x}_s\,dp\right\}\mathbf{B}_s''}} \quad (44)$$

Since the polynomial coefficients are constants with respect to each layer, the diagnostic model may be expressed as

$$G = \sum_{s=1}^{7} C_s\,\overline{\overline{\mathbf{A}_s''^T\,\mathbf{X}_s\,B_s''}} \quad (45)$$

where the constant C_s for an atmospheric layer is

$$C_s = \frac{p_{0s}^{R\overline{\overline{\Gamma}}_s/g}}{(1-\overline{\Gamma}_s/\Gamma_d)\overline{T}_{0s}\,c_{2s}} \quad (46)$$

and the elements x_{ij} of the $(k+1)\times(q+1)$ matrix, $\mathbf{X}_s$, are

$$x_{ij} =$$

$$\sum_{l=0}^{(i+j-3)}\frac{(i+j-3)!\,(j-1)\,(C_{2s})^{3-(i+j)}\,(-C_{1s})^l}{l!\,[(i+j-3-l)!\,[(i+j)-(2+l+(R\overline{\Gamma}_s/g))]}$$

$$\times\,[p^{(i+j)-(2+l+(R\overline{\overline{\Gamma}}_s/g))}]_{p_{s+1}}^{p_s} \quad (47)$$

The integral solution of (45) may be time-averaged to yield the generation due to the infrared component of heating. The resulting expression may be partitioned among the three scales of atmospheric circulation by substituting the time-averaged form of (45) into equation (9).

$$\overline{G} = \sum_{s=1}^{7} C_s\left\{\overline{\overline{[\overline{\mathbf{A}}]_s''\,\mathbf{X}_s[\overline{\mathbf{B}}]_s''}} + \overline{\overline{\overline{\mathbf{A}}_s^*\,\mathbf{X}_s\,\overline{\mathbf{B}}_s^*}} + \overline{\overline{(\mathbf{A}')_s''\,\mathbf{X}_s(\mathbf{B}')_s''}}\right\} \quad (48)$$

The advantages of expressing the generation in this form are: (1) the vertical description of both temperature and heating allow the generation to be estimated as a function of pressure, (2) a variable static ability can be used in the integration model, and (3) the diagnostic model provides unbiased estimates of the zonal and eddy generation (Appendix V, Johnson, 1965).

The most serious limitation of this study is the small data sample. The thirteen radiometersonde stations represent a limited area, the eastern half of the United States and the Caribbean. Thus, the estimates based on these thirteen stations represent only a contribution to the global generation integral. On the other hand, studies involving only data from limited areas have advantages. For example, if one wishes to study the contribution of the smaller scales which might be contained within the data region, many of the physical processes expressed by the covariant terms in Lorenz's equations will attain their maximum values. When only two or three of these features are averaged with other comparatively quiescent features of the atmosphere, one underestimates the importance of the small scale features.

Furthermore, when working with a limited data sample, it is important that a diagnostic model be used which maximizes the information which can be extracted from two observational series. As is shown in Appendix V of the original thesis, unbiased polynomial estimates of the temperature and heating provide an unbiased estimate of the generation integral. Thus, with the increased resolution of this model it is possible to investigate the contributions of the smaller scale features of the atmosphere in which the spatial variability of the meteorological variables is great.

In evaluating the above equations, C_s and the integrated matrix, $\mathbf{X}_s$, are constants for a given layer. The necessary constants to determine C_s and $\mathbf{X}_s$ are presented in Table 3. In these computations the static stability of the US Standard Atmosphere was used. For this reason the upper surface of level four was placed

Table 3. *Constants for* C_s

Layer	$p_s - p_{s+1}$ (mb)	p_{0s} (mb)	$\overline{\overline{T}}_{0s}$ (°K)	Γ_s (°C/km)	c_{1s} (mb)	c_{2s} (mb)
1	1000–800	1000	288	6.5	900	100
2	800–600	800	275	6.5	700	100
3	600–400	600	261	6.5	500	100
4	400–234	400	241	6.5	317	83
5	234–100	234	218	0	167	67
6	100– 50	100	218	0	75	25
7	50– 25	50	218	0	37.5	12.5

$\Gamma_d = 9.8$°C/km. $g = 980$ cm/sec^2. $R = 2.87 \times 10^6$ ergs/gm-deg.

at 234 mb, which is the tropopause of the US Standard Atmosphere.

Since the atmosphere was divided into seven layers, the seven C's and X's of equation (48) are determined for each level and stored in the computer, thus facilitating the integrations.

To determine the stationary zonal generation, it was necessary to determine zonal mean profiles of temperature and cooling. This was done by dividing the thirteen stations into three zonal rings surrounding their latitude. This division by ring numbers is presented in Table 1. The stationary zonal component was computed for each ring and the ring averages used to obtain an average zonal generation. The transient and stationary eddy components were computed for each station and the station averages were used to obtain averages for each zonal ring and also for the entire area. A total generation was obtained from the sum of all three components.

5. Results

Estimates of the transient, stationary eddy and stationary zonal generation of available potential energy obtained by the polynomial integration method are presented in this section. As noted before, these estimates are from a limited area and must be regarded as only a contribution to the global value of the generation of available potential energy. The estimates, which represent the contribution from a continental region within the westerlies (Zones I and II) and from a maritime area of the subtropics (Zone III), are presented in Tables 4–8.

For convenience of discussion, the estimates for the seven layers of integration are combined to form three layers. The first layer extends from the 1000 to the 600 mb surface, thus representing the lower half of the troposphere. The second layer, 600 to 234 mb, represents the upper troposphere, and the third layer, 234 to 25 mb, the stratosphere. Hereafter, the layers will be simply noted as the lower tropospheric, upper tropospheric, and stratospheric layers.

Table 4 gives the estimates of the transient generation. A comparison of the three layers reveals that the mean transient estimate of Zones I, II and III is negative for the lower troposphere (-0.47×10^{-3} watts/m^2-mb), while it is a small positive quantity for the other two layers ($+0.14$ watts/m^2 – mb for the upper troposphere and $+0.10$ watts/m^2 – mb for the stratosphere). The results indicate that during this limited period the phase of the temperature and infrared heating field reversed between the lower troposphere and the upper two layers. This variation of the generation with height will be further discussed after the generation at individual stations is considered.

An examination of the total transient generation in a unit column for each station (Table 4) indicated that contributions are predominantly negative. However, considerable variation in the estimates exists between stations. For example, large positive values are found at Miami ($+0.70$ watts/m^2) and Curacao ($+0.41$ watts/m^2), Zone II and III stations, while large negative values are found at Madison (-1.09 watts/m^2) and Peoria (-0.95 watts/m^2), both Zone I stations. The difference between the generation estimates of the higher latitude stations and the low latitude stations is very likely related to the persistence of certain synoptic events during the data period.

Since these data involve time averages, they do not describe time variations of the generation by individual transient disturbances. Thus, one of the perplexing questions which the study cannot entirely resolve is how the generation varies during the life cycle of a transient disturbance. From certain physical arguments based on the distribution of clouds (see Section 2), it appears that the contribution is positive during the incipient, developing and mature stage of the disturbance and negative during its dissipating stage. Although exact estimates cannot be made, some information concerning this postulate can be obtained by inspecting the

Table 4. *Transient generation*

Units: Layers—10^{-3} watts/m^2 mb. Total—watts/m^2

Zone I						
Station ...	405	532	641	645	747	Average
Layer (mb)						
1000–600	−2.67	−1.91	−1.39	1.00	− .01	−.99
600–234	.84	− .39	−1.29	− .23	− .40	−.30
234– 25	.02	− .12	− .17	.18	1.13	.21
Total	− .77	− .95	−1.09	.36	.09	−.47
Zone II						
Station ...	202	226	363			Average
Layer (mb)						
1000–600	1.30	− .33	−1.65			−.23
600–234	.36	.45	.93			.58
234– 25	.14	− .21	.64			.19
Total	.70	− .11	− .17			
Zone III						
Station ...	383	525	866	967	988	Average
Layer (mb)						
1000–600	− .59	− .14	−1.00	.27	− .05	−.30
600–234	.56	− .72	− .09	− .34	.89	.06
234– 25	.36	−1.66	.52	− .08	.56	−.06
Total	.04	− .68	− .33	− .03	.41	−.12
Grand average–Zones I, II, III						
Layer (mb)						
1000–600	−.47					
600–234	.14					
234– 25	.10					
Total	−.13					

daily contribution of each station to the time averaged transient generation (see Table 5). One notes that there is considerable variation in the daily estimates, which confirms that the time averaged estimate of the generation is not the result of the sum of relatively uniform contributions. The best indication that the covariance of temperature and infrared cooling reverses sign is given by the period of 13 January through 17 January. The sums of the estimates for the U.S. stations for each day clearly indicate that during this period the estimates were consistently positive. At this time the eastern continental United States was under the influence of a well developed middle tropospheric trough and two surface lows, one of which moved eastward along the U.S.—Canadian border and the other eastward along the Gulf Coast. Evidently, within these traveling disturbances, the cloud distribution and thermal structure were such that the contribution by the eight U.S. stations was predominantly positive. It appears, as suggested in Section Two, that the extensive cloudiness in the warm air reduces the cooling by the infrared component while the cooling within the clear cold air is a maximum, thus producing a positive contribution to the generation of available potential energy.

It was also noted in Section 2 that above the level of the clouds a negative contribution is likely to occur. An inspection of the daily contribution by each of the seven layers revealed that in many cases the sign of the individual layers reverses one or more times. The result is probably due to the horizontally stratified nature of clouds and water vapor. In the presence of several layers of clouds, the relative cooling changes sign at the top of each cloud layer. Since within individual airmasses the lapse rate of temperature is nearly constant throughout the tropopshere, the relative temperature deviation is constrained to be either

Table 5. *Daily contributions*

Units:

Station	December										
	20	21	22	23	24	25	26	27	28	7	8
202									−.70	1.17	.32
226		−.82	−2.88	3.26			1.27		1.33	.05	.79
405	.02	1.74	.31	−.11	−7.78		−.41	1.66	−.95	−4.45	−3.21
363			−.48		−.84	.51	.27			−.24	−.31
532	−.82		−6.31	−4.45	−1.83	.81				−4.28	1.16
641				−1.95					.15		
645											
747	1.34	−.04	−3.96	.13	.61	−1.08			3.53	−1.53	3.77
Daily sub-zone I & II Total	.28	.29	−2.66	−2.62	−2.46	.08	.38	1.66	.67	−1.55	.42
383	.23	.73	.45	1.66	−1.06	−3.62	3.55	−7.46	1.03	.78	.56
525		.55	4.92	−3.21	1.75	−2.30	−2.94	−3.00		.45	−1.99
866	−.92	.23	−2.27	−1.70	−2.00		−3.58	6.42	−1.15		.34
967			.76	−1.40	−.26		−3.08	.72	1.65		
988	−.93	.70	1.68	−.87	−.89	−1.87	−1.60	4.60	.45		.47
Daily sub-zone III Total	−.54	.55	1.95	−1.10	−.49	−2.59	−1.51	.25	.49	.61	−.15

a positive or negative quantity while the sign of the heating deviation changes at the top of each cloud layer. Thus, the generation contribution also reverses sign at the top of each cloud layer. For example, at Miami on January 14, 1960, the following generation values were obtained for the seven layers:

Layer (mb)	Transient generation (10^{-3} watts/m^2 mb)
1000–800	.82
800–600	− .22
600–400	3.41
400–234	− .25
234–100	.17
100– 50	− .48
50– 25	−1.38

Evidently tops of cloud layers were found at approximately 800 mb, 400 mb and 100 mb. The radiosonde data for that day verifies the existence of moist layers, possibly clouds, at the lower two heights. The humidity observations are missing at the upper level. Large vertical variations of generation such as these indicate that studies using mean values of cooling for atmospheric columns (such as those required when satellite data are employed) may be appreciably constrained. An alternative method which has been presented by Smith, Horn & Johnson (1966) uses satellite data to estimate the cooling within different atmospheric layers. Such a method may be a valuable technique in estimating the infrared generation on a global scale. There are cloud distributions, however, where the generation will be positive throughout the entire atmospheric column. Consider, for example, a case in which the top of the cirrus shield reaches a height equal to the height of the intersection of the polar and tropical soundings. Although the differential heating field is reversed above this level the temperature field of horizontal deviations also reverses sign, causing a positive generation throughout the column. Such an example occurred on 23 December, 1960, at Montgomery where all levels were positive except the 100–50 mb level. The total estimate for the column was 3.26 watts/m^2.

Large positive contributions can also be obtained from cloudless regions. These situations occur when there is large infrared cooling from the cold, dry tropospheric air associated with a recent polar outbreak. Under such conditions the generation may be positive throughout the atmospheric column, for the polar stratosphere may be experiencing relative warming with respect to the colder subtropical stratosphere.

to transient generation

Watts/m²

January											
9	10	11	12	13	14	15	16	17	18	19	20
.71		.56	-1.48	.45	.74		2.02				
.20	-4.29	.43	-1.55		.88	3.03	.34	-.60	-1.38	-.05	
.08	-6.52	1.40	-2.44	-.22	.15	4.87		.19	1.32		
-.10	-1.82	-.63			2.43	-.24	-1.17	-.98	-2.03	1.46	
-.46	.38	1.97	-1.65	-2.66	-.60	2.36		.21	1.60		
-.34		-.58	-3.06	.72							
				-.72	1.11	-.91	4.85	.40	.99	-1.36	-.06
-.53	3.92	-2.55	-1.43	-2.31	.11	.55	.69	3.20	-5.16		
-.06	-1.66	.09	-1.93	-.79	.69	1.53	1.29	.39	-.78	-.02	-.06
-.88	-.78	-.88	1.19	1.02	.54	.56	1.22	-.34			
-.96	-1.16	-.58			-2.24	-1.19	.98	-1.62	.57	.30	-1.98
-3.68	3.27	1.81	.17	1.43	-2.44	-.03	.52				
		1.72	.96	.02			-1.27	-.07			
	-.99	5.75	.55	.75		.20	-.27	.29	-.10		
-1.84	.09	1.36	.72	.81	-1.38	-.14	.24	-.49	.24	.30	-1.98

The relative warming in the polar stratosphere is produced by direct absorption of the upward radiative flux from the troposphere. At the tropopause the value of the upward radiative flux from the cold clear polar troposphere is significantly greater than the upward radiative flux emitted from regions with high clouds (or moisture layers). Thus, a positive contribution to the generation of eddy available potential energy may again occur throughout the atmospheric column.

An example which illustrates the large generation that can be achieved in fresh polar air and the rapid changes in generation which occur as the air mass is modified is given by the data for International Falls. On 10 January 1961, International Falls experienced a large positive generation (3.92 watts/m²) while under the influence of an anticyclone associated with a recent outbreak of polar air. On the following three days, the generation became negative (-2.55, -1.43, -2.31 watts/m², respectively). An examination of synoptic charts for this period revealed that the cold polar air stagnated over the eastern United States and warmer more moist air was advected above it. The higher clouds, which resulted, greatly reduced the infrared cooling; and as a consequence, the generation became negative. Although the mean transient generation for the entire area was -0.13 watts/m² the spatial and time variations of the generation noted above indicate that this term may be either a significant source or sink of available potential energy in specific cases. The range of the transient generation estimates in Table 5 is slightly larger than the range of frictional dissipation within the planetary boundary layer for light and moderate winds over the forested region of Northern Wisconsin (W. B. Johnson, 1965). It appears that in an energetically consistent numerical model where frictional dissipation is included, infrared cooling at the scale of the secondary circulation should also be incorporated. Consequently, the time and space variations of the transient generation should be further investigated for individual synoptic events.

The estimates of contributions to the stationary eddy generation are presented in Table 6. The total contribution from the entire area is -0.08 watts/m², thus indicating that the stationary eddy component is not a large sink of available potential energy. The mean estimate for the stratospheric layer is considerably more negative than the mean estimate for the tropospheric layers. This indicates that at this scale

Table 6. *Stationary eddy generation*

Units: Layers—10^{-3} watts/m^2 mb. Total—watts/m^2

Zone I						
Station ...	405	532	641	645	747	Average
Layer (mb)						
1000–600	– .39	– .03	.32	– .62	–1.97	– .54
600–234	– .21	– .25	– .02	– .48	.00	– .19
234– 25	.21	.00	– .06	– .68	.50	.00
Total	– .10	– .11	.11	– .58	– .70	– .29
Zone II						
Station ...	202	226	363			Average
Layer (mb)						
1000–600	8.74	–7.79	2.56			1.16
600–234	.91	.31	–1.46			– .69
234– 25	.84	–.58	– .30			– .57
Total	3.06	–3.21	.44			.10
Zone III						
Station ...	383	525	866	967	988	Average
Layer (mb)						
1000–600	– .32	– .13	.06	.03	– .36	– .14
600–234	.00	.26	.12	.21	.61	.24
234– 25	– .55	– .29	.19	–2.21	.03	– .56
Total	– .25	– .02	.11	– .38	.09	– .09
Grand average						
Layer (mb)						
1000–600	.19					
600–234	– .20					
234– 25	– .41					
Total	– .08					

the stratospheric cooling by infrared radiation is proportional to the stratospheric temperature and is not significantly influenced by factors such as clouds, water vapor and dust. On the other hand, the positive estimate (0.10 watts/m^2 mb) of the transient generation for the stratospheric layer indicates that there are variations in absorbing constituents in the stratosphere associated with transient disturbances.

Further examination of Table 6 reveals that a large positive generation (1.16 watts/m^2-mb) exists for the lower troposphere of Zone II. This estimate can be misleading because it is in part the result of the difference in the latitude of Miami and the other two stations in the zone. Since computation of the stationary eddy generation involves the product of deviations of the time averaged temperature and cooling profiles from their respective zonal means, the temperature deviation of Miami was unusually large because of the mean north-south temperature gradient. Combined with the large positive deviation was an appreciable relative heating term due to extensive cloudiness in this area. On the other hand, Montgomery had a large negative temperature deviation and a positive heating deviation, thus a large negative estimate. It is interesting to note that although these large temperature deviations are due to the thirteen degree latitudinal extent of the zonal ring, the deviations of the stationary eddy temperature field within a unit zonal ring have the same magnitude as the deviations within Zone II. In view of this fact, it is probable that the range of the contributions (both positive and negative) from different stationary features (continents and oceans) within any unit zonal ring is as great as the difference between Miami and Montgomery. This should be particularly true in the latitudinal belt of 20° to 30° N, where the subtropical highs are most pronounced and in which the temperature field and cloud and water vapor tend to have a systematic distribution.

Although from this study it is not possible to estimate the global averaged stationary generation, the implications of the large positive and negative values for the stationary generation of Zone II are interesting in view of Murakami's (1960) results. Murakami postulates that, if the stationary disturbances transfer available potential energy to the transient disturbances, "the available potential energy of the stationary disturbances should be supplied by the nonadiabatic process of warming of warm air and cooling of cold air". He also notes that the two most probable diabatic components which might generate the available potential energy were infrared heating and sensible heat transfer, since his generation estimate for the latent heat component was an order of magnitude less than the required generation at this scale. The results obtained here tend to indicate that the infrared generation, either positive or negative, by the stationary disturbances may be important.

In Table 7 the estimate of the stationary zonal generation is -1.92 watts/m², a large negative value. Shen's (1963) zonal generation estimate for the infrared component from the use of satellite data was -1.75 watts/m² for portions of the period of December, 1959, through February, 1960. Thus the two estimates of zonal generation for the winter hemisphere are nearly equal. One notes that the principal sink of zonal available potential energy occurs within the lower tropospheric layer, -4.13 watts/m²-mb. Within the upper tropospheric and stratospheric layers, the negative generation estimate is an order of magnitude less, -0.41 and -0.35 watts/m²-mb, respectively. This difference between the lower and higher portions of the atmosphere is due to the strong meridional temperature gradient which exists in the lower troposphere during this period. Since the Caribbean tends to be less cloudy than the higher latitudes during this season, the warmer subtropics experienced greater infrared cooling than the polar air over the U.S.

The zonal generation estimate in pressure coordinates of -1.92 watts/m² is in striking contrast with the zonal generation estimate in isentropic coordinates of 1.61 watts/m² based

Table 7. *Stationary zonal generation*

Units: Layers—10^{-3} watts/m² mb. Total—watts/m²

Zone	I	II	III	Average
Layers (mb)				
1000–600	−12.47	−2.40	.53	−4.13
600–234	−.64	.13	−.74	−.41
234–25	−.43	.21	−.80	−.35
Total	−5.44	−.89	−.24	−1.93

on equation (1) by Dutton & Johnson (1967). The difference in the two results is that the effect of net heating at high pressure and net cooling at low pressure is retained in the isentropic coordinate expression but not in the approximate zonal generation expression in pressure coordinates. The two results can be compared by considering the neglected term of equation (2) involving the effect of net heating on a pressure surface. Lorenz's Figure 2 (1960) presents a meridional distribution of N which shows that the pressure average value, $\bar{N}$, will be negative at nearly all levels in the atmosphere. In equation (2), the generation due to net heating is proportional to the product of N and $\overline{\overline{Q}}$. Since the infrared component of $\overline{\overline{Q}}$ is also negative at all pressure levels, the product of $\overline{\overline{N}}$ and $\overline{\overline{Q}}$ is greater than zero at nearly all levels. Thus the infrared component of net heating generation is undoubtedly positive. If the result presented in this paper is to be compatible with the result of Dutton & Johnson (1967), it is quite likely that the infrared contribution of this term will more than offset the negative zonal generation estimate of this study and that in studies which include the net heating, zonal and eddy components the generation due to infrared processes will be approximately $+1.0$ to 2.0 watts/m². In the future the neglected net heating term should be incorporated in generation studies using pressure coordinates or the studies should be conducted in isentropic coordinates which retain the effect of net heating. This and other advantages of conducting available potential energy studies in isentropic coordinates are presented by Dutton & Johnson (1967).

The results of Table 4–7 are summarized in Table 8. One notes that there is a reversal of sign between the lower tropospheric layer and the two higher layers in both the transient and

Table 8. *Transient, stationary eddy, stationary zonal, and average infrared generation*

	Transient	Stationary eddy	Transient + sta. eddy	Stationary zonal	Total
Layers (mb)					
1000–600	−.47	.19	−.28	−4.13	−4.41
600–234	.14	−.20	−.06	−.41	−.47
244–25	.10	−.41	−.31	−.35	−.66
Total	−.13	−.08	−.21	−1.92	−2.13

stationary eddy estimates. However, one cannot necessarily conclude that this is a representative feature of globally averaged generation estimates for these two scales. Within a different time period the results may be quite different for this area, because of different cloud distributions within these two scales.

A subtotal of the transient and stationary eddy contribution is given in the third column. Within the limitations of the study the subtotal is the best approximation to the time averaged infrared eddy generation. The stationary zonal subtotal may be considered as an approximation of the zonal infrared generation. Although the mean generation due to infrared radiation is negative, the large differences between the stationary zonal and transient eddy subtotal stand out, as expected. As noted previously, the small negative values found in the subtotal are the result of the inclusion of a number of significantly positive and negative estimates at these scales.

Another feature presented in the total generation estimate in the fifth column of Table 8 is the pronounced differences in the higher layers. These results indicate that large vertical variations of the infrared generation exist and may be an important feature in different scales of the atmosphere's circulation.

6. Conclusions and suggestions for future research

In this study estimates of the generation of zonal and eddy available potential energy have been obtained for a limited area, thus they represent a contribution to the average global generation. To obtain these estimates, a diagnostic model with increased resolution and reliability was developed in which the temperature and heating profiles were described by individual approximating polynomials. A technique for integrating the product of the approximating polynomials was devised. As a consequence it was possible to describe the vertical variation of the generation within the scale of the secondary circulation.

The following conclusions may be made concerning the generation of available potential energy:

1) The zonal and eddy generation during the data period for the limited area was negative. Future studies of the generation of available potential energy should incorporate the effect of net heating on a pressure surface to establish its magnitude.

2) While the stationary zonal generation was a large negative value, the transient and stationary eddy values were only slightly negative.

3) An analysis of the daily values indicates that the transient and stationary eddy generations vary considerably from day to day and at times may attain either significantly positive or negative values.

4) There are pronounced vertical variations in the generation of available potential energy. In general, the extreme values—both positive and negative—occur in the lower troposphere. This is undoubtedly the result of varying distributions of cloudiness and water vapor. In individual cases the sign of the generation reverses between different atmospheric layers depending on the distribution of clouds.

5) Because of the large daily variations as well as vertical variations, it appears that additional intensive studies of the generation for local disturbances should be undertaken. In the life cycle of a disturbance, the infrared generation, both positive and negative, is very likely an important consideration.

6) The range of the transient generation estimates was slightly larger than the range of frictional dissipation estimates within the planetary boundary layer for light and moderate winds. Consequently, the estimates of infrared cooling should be considered as necessary information for any future numerical model which includes boundary layer frictional dissipation.

Although the goal of the thesis was a study of the generation of available potential energy and, in particular, its vertical variation, a number of serendipitous results were attained. The referenced appendixes are available in the original thesis filed with the Memorial Library, University of Wisconsin. They include:

7) The variance of the downward, upward, and net radiative flux measured by the radiometersonde was firmly established for the first time (Johnson, 1966 and Appendix I).

8) Approximating polynomials were applied to radiometersonde data to obtain continuous cooling profiles which possess a RMS error of only ± 0.22°C/day, as opposed to the previous RMS error of ± 0.34°C/day for a 100 mb atmospheric layer. The success achieved by approximating polynomials suggests that they may be more widely used in diagnostic studies to determine vertical derivatives of other meteorological variables, such as wind, temperature, etc.

9) A technique which permits the integration of two approximating polynomials was developed. It was shown that this method provides unbiased integral estimates when the two approximating polynomials are unbiased and the observational error components are independent (see Appendix V).

Acknowledgments

I am grateful to Professor Lyle H. Horn for his encouragement and guidance during the preparation of this thesis. I also wish to express appreciation to Professors Verner Suomi, Heinz Lettau and Irwin Guttman for their assistance at various stages. I gratefully acknowledge the invaluable role of Mr. Charles Hutchins in preparing the computer programs and processing the data and the assistance of Dr. Peter M. Kuhn in making available the radiometersonde data.

REFERENCES

Air Weather Service Technical Report 105–133, 1955. Accuracies of Radiosonde Data. Air Weather Service (MATS), United States Air Force, Washington, D.C.

Brewer, A. W. & J. T. Houghton, 1956. Some Measurements of the Flux of Infra-red Radiation in the Atmosphere. *Proceedings of the Royal Society, Series A*, *236*, 175–176.

Brown, J. A. 1964. A Diagnostic Study of Tropospheric Diabatic Heating and the Generation of Available Potential Energy. *Tellus 16*, No. 3, 349–366.

Bushnell, Robert H. 1962. *An investigation of the Problem of the Measurement of Infrared Radiation in the Lower Stratosphere.* Ph. D. thesis, Department of Meteorology, University of Wisconsin.

Clapp, P. F. 1961. Normal Heat Sources and Sinks in the Lower Troposphere in Winter. *Monthly Weather Review 89*, No. 5, pp. 147–162.

Clapp, P. F. & F. J. Winninghoff, 1963. Tropospheric Heat Sources and Sinks at Washington, D.C., Summer 1961, Related to the Physical Features and Energy Budget of the Circulation. *Monthly Weather Review 91*, No. 10, 494–504.

Corcoran, J. L. & L. H. Horn, 1964. The Role of Synoptic Scale Variations of Infrared Radiation in the Generation of Available Potential Energy. *Journal of Geophysical Research 70*, No. 18, 4521–4527.

Dutton, J. A. & D. R. Johnson, 1967. The Theory of Available Potential Energy and a Variational Approach to Atmospheric Energetics, *Advances in Geophysics 12*, 333–463, Academic Press, New York.

Ferrel, W., 1889. *A Popular Treatise on the Winds.* John Wiley and Sons, New York.

Gergen, J. L. 1956. Black ball: Device for Measuring Atmospheric Infrared Radiation. *Review of Scientific Instruments 27*, No. 7, 453–460.

Hadley, G., Concerning the Cause of the General Tradewinds. *Phil. Trans. Roy. Soc. London. 39*, No. 58, 1735–36. Reprinted in "The Mechanics of the Earth's Atmosphere. A Collection of Translations by Cleveland Abbe," 3rd Collection, *Smithsonian Misc. Coll. 51*, No. 4, 1910.

Hildebrand, Francis B. 1956. *Introduction to Numerical Analysis.* McGraw-Hill, New York.

Jeffreys, H. 1933. The Function of Cyclones in the General Circulation. *Procès-Verbaux de l'Association de Météorologie*, UGG (Lisbon), Part II (Mémoires), 219–230.

Johnson, Donald R. 1965. *The Role of Terrestrial Radiation in the Generation of Available Potential Energy.* Ph. D. Thesis, Department of Meteorology, University of Wisconsin.

Johnson, Donald R. 1966. The Effect of Bias and Random Radiometersonde Temperature Errors in the Estimation of Atmospheric Downward, Upward, Net and Equivalent Infrared Irradiance. *Journal of Geophysics 71*, No. 24, 5815–5826.

Johnson, W. B. 1965. *Atmospheric Boundary Layer Dynamics Over the Forests of Northeastern Wisconsin.* Ph. D. Thesis, Department of Meteorology, University of Wisconsin.

Kendall, Maurice G. & A. Stuart, 1958 & 1961. *The Advanced Theory of Statistics*, London, C. Griffin; *Distribution Theory*, 1958, Vol. 2, *Statistical Inference and Statistical Relationship*, 1961.

Korb, G. & F. Möller, 1962. *Theoretical Investigations of Energy Gain by Absorption of Solar Radiation in Clouds.* Ludwig-Maximilian-Universität, Meteorologisches Institut, München, Germany, Contract DA-91-591-EUC-1612.

Kuhn, P. M. 1961. Accuracy of the Airborne Economical Radiometer. *Monthly Weather Review 89*, No. 8, 285–287.

Kuhn, P. M. & D. R. Johnson, 1966. Improved Radiometersonde Observations of Atmospheric Infrared Irradiance. *Journal of Geophysical Research 71*, No. 2, 367–373.

Kuo, H. L. 1956. Energy Releasing Processes and Instability of Thermally Driven Motions in a Rotating Fluid. *J. Meteor. 13*, 561–568.

Kuo, H. L. 1957. Further Studies of Thermally Driven Motions in a Rotating Fluid. *J. Meteor. 14*, 553–558.

Lorenz, E. N. 1955*a*. Available Potential Energy and the Maintenance of the General Circulation. *Tellus 7*, 157–167.

Lorenz, E. N. 1955*b*. Generation of Available Potential Energy and the Intensity of the General Circulation. In "*Large Scale Synoptic Processes*" (J. Bjerkness, Project Director), Department of Meteorology, Final Report, 1957, Contract AF 19(604)-1286. University of California, Los Angeles, California.

Lorenz, E. N. 1960. Generation of Available Potential Energy and the Intensity of the General Circulation. *Dynamics of Climate* (R. L. Pfeffer, ed.), 86–92. Pergamon Press, New York.

Margules, M. 1903. Über die Energie der Stürme. Translated in *Smithsonian Miscellaneous Collections. 51*, 1910.

Murakami, T. 1960. On the Maintenance of Kinetic Energy of the Large-Scale Stationary Disturbances in the Atmosphere. Massachusetts Institute of Technology, Department of Meteorology, *Scientific Report No. 2, Planetary Circulations Project*, Contract No. AF 19(604)-6108.

Oort, Abraham H. 1964. On estimates of the atmospheric energy cycle. *Monthly Weather Review 29*, No. 11, 483–493.

Palmén, E. 1959. On the Maintenance of Kinetic Energy in the Atmosphere. *The Atmosphere and the Sea in Motion.* Ed. by B. Bolin, New York, 212–223, The Rockefeller Institute Press.

Plackett, R. L. 1960. *Principles of Regression Analysis.* Clarendon Press, Oxford.

Rossby, C. G. 1941. "The Scientific Basis of Modern Meteorology," *Climate and Man: Yearbook of Agriculture.* United States Dept. of Agriculture, Government Printing Office, Washington, 599–654.

Rossby, C. G. 1949. On a Mechanism for the Release of Potential Energy in the Atmosphere. *Journal of Meteorology 5*, 163–180.

Shen, W. C. 1963. *The Generation of Available Potential Energy Due to Horizontal Variations in Terrestrial Radiation as Measured by the Satellite Explorer VII.* Ph.D. Thesis, University of Wisconsin.

Smith, W. L., L. H. Horn & D. R. Johnson, 1966. TIROS Radiation Measurements and the Infrared Cooling of the Atmosphere. *Journal of Applied Meteorology 5*, No. 4, 526–531.

Starr, V. P. 1948. An Essay on the General Circulation of the Earth's Atmosphere. *Journal of Meteorology 5*, 39–43.

Starr, V. P. 1956. Modern Developments in the Study of the General Circulation of the Atmosphere. *Journal of Geophysics Research 61*, 334–340.

Starr, V. P. 1958. What Constitutes Our New Outlook on the General Circulation? *Journal of the Meteorological Society of Japan*, Series II, *36*, No. 5, 167–173.

Sabatini, R. R. & V. E. Suomi, 1962. On the Possibility of Atmospheric Infrared Cooling Estimates from Satellite Observations. *Journal of Atmospheric Science 20*, No. 1, 62–65.

Suomi, V. E. & W. C. Shen, 1963. Horizontal Variations of Infrared Cooling and the Generation of Eddy Available Potential Energy. *Journal of Atmospheric Science 20*, No. 1, 62–65.

Wiin-Nielsen, A. & J. A. Brown, Jr., 1962. On Diagnostic Computations of Atmospheric Heat Sources and Sinks and the Generation of Available Potential Energy. *Proceedings of the International Symposium on Numerical Weather Prediction, Meteorological Society of Japan, Tokyo*, 519–613.

РОЛЬ ТЕПЛОВОГО ИЗЛУЧЕНИЯ ЗЕМЛИ В ГЕНЕРАЦИИ ЗОНАЛЬНОЙ И ТУРБУЛЕНТНОЙ ДОСТУПНОЙ ПОТЕНЦИАЛЬНОЙ ЭНЕРГИИ

Из 198 полетов радиометрических зондов, проведенных на тринадцати станциях, расположенных в восточной половине США и бассейне Карибского моря, получены осредненные по времени оценки генерации в атмосфере зональной и турбулентной доступной потенциальной энергии инфракрасным излучением. По полю температуры и данным о притоке радиации вертикальные профили температуры и охлаждения атмосферы по отдельности оценены с помощью полиномов, аппроксимирующих в смысле метода «наименьших квадратов». С целью получить осредненные по времени корреляции профилей охлаждения и температуры для каждого из семи рассматриваемых слоев атмосферы была развита методика интегрирования полиномов. Осредненные по времени оценки для каждаго из семи слоев атмосферы разделяются на переходную, стационарную турбулентную и стационарную зональную компоненты. Результаты указывают, что все они являются стоками для доступной потенциальной энергии со следующими оценками: для переходной компоненты −0,13 ватт/м², для стационарной турбулентности −0,08 ватт/м², и для стационарной зональной −1,92 ватт/м². Анализ суточных величин показывает, что генерация переходной компоненты значительно изменяется день ото дня и временами достигает больших положительных или отрицательных величин. Интервал изменений оценок генерации переходной компоненты немного больше, чем интервал измене-

ний оценок величин диссипации за счет трения в планетарном пограничном слое для слабых и умеренных ветров. Имеются заметные вертикальные вариации в оценках генерации с предельными значениями, как положительными, так и отрицательными, встречающимися в нижней тропосфере. Это, несомненно, является следствием меняющегося распределения облачности и водяного пара. Поскольку имеются большие суточные вариации, так же как и вертикальные вариации, то очевидно, что должно быть проведено дополнительные широкое изучение генерации для локальных возмущений. Обсуждается влияние генерации инфракрасной радиации, возникающей вследствие нагревания, на изобарическую поверхность.